

**Electronic Supporting Information (ESI)**  
**for**

**A naphthalene anhydride derivative as multi-modal probe for trace water detection and lipid droplets/lysosomes imaging**

Peng Ye<sup>a,b,c</sup>, Haitao Zhang<sup>a,b,c\*</sup>, Jianbo Qu<sup>a,b,c</sup>, Xiuzhong Zhu<sup>a,b,c\*</sup>, Qingfei Hu<sup>a,b,c</sup> and Shanghong Ma<sup>a,b,c</sup>

<sup>a</sup> State Key Laboratory of Biobased Material and Green Papermaking, Qilu University of Technology (Shandong academy of sciences).

<sup>b</sup> Faculty of Light Industry, Qilu University of Technology (Shandong academy of sciences).

<sup>c</sup> Key Laboratory for Green Leather Manufacture Technology of China National Light Industry Council, Faculty of Light Industry, Qilu University of Technology (Shandong academy of sciences).

\* Correspondence: zhanghaitao@qlu.edu.cn (H.Z.). Tel.: +86-133-6531-6033 (H.Z.); zhuxiuzhong321@163.com (X.Z.). Tel.: +86-187-0687-6564.

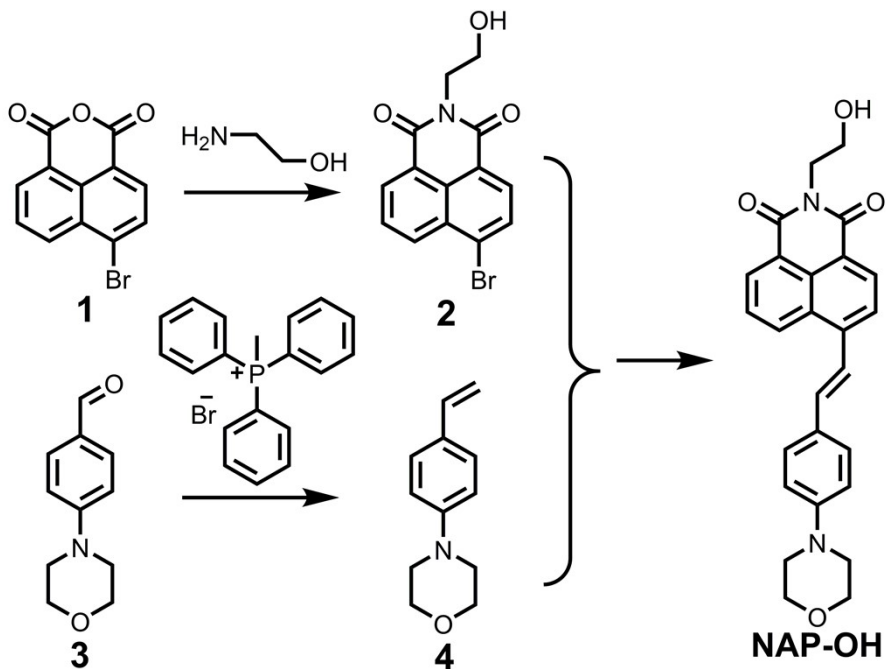
## Table of Contents

- 1. Materials and measurements.**
- 2. Synthesis and Characterization of NAP-OH.**
  - 2.1 Synthesis of 6-bromo-2-(2-hydroxyethyl)-1,8-naphthalimide (compound 2)**
  - 2.2 Synthesis and characterization of 4-(4-vinylphenyl) morpholine (compound 4)**
  - 2.3 Synthesis and characterization of NAP-OH**
- 3. The theoretical calculation**
- 4. Determination water contents in various samples.**
  - 4.1 Fluorescence emission spectroscopic studies of NAP-OH in organic solvents containing different amounts of water.**
  - 4.2 Determination of detection limit of NAP-OH toward water in organic solvents.**
  - 4.3 Reproducibility of the sensor in 0.5% (v/v) H<sub>2</sub>O/1,4-Dioxane.**
- 5. Cell co-staining experiments.**

## 1. Materials and measurements

All reagents and solvents were obtained from commercial sources without further purification.  $^1\text{H}$  NMR and  $^{13}\text{C}$  NMR spectra were obtained from an AVANCE II 400 nuclear magnetic resonance apparatus, respectively. Tetramethylsilane (TMS) or solvent peaks were used as internal standards. High-resolution mass spectra in ESI+ mode were recorded on a Bruker MicroTOF-Q III mass spectrometer. All UV-Vis absorption and emission spectra were obtained from Shimadzu UV-2600 spectrometers and Shimadzu RF-5301PC spectrometers, respectively. A KF titrator model 831 KF based on coulometric Karl Fischer titration was used for the detection of water content in the samples. During cell imaging experiments, fluorescence imaging pictures were recorded from a Leica TCS SP8 confocal laser scanning microscope and images were processed using LAS-AF. Density functional theory (DFT) calculations were performed using the Gaussian 09w package.

## 2. Synthesis and Characterization of NAP-OH.



Scheme S1. Synthesis procedure and structures of NAP-OH.

## 2.1 Synthesis of 6-bromo-2-(2-hydroxyethyl)-1,8-naphthalimide (compound 2)

Compound **1** 4-bromo-1,8-naphthalenedicarboxylic anhydride (20 mmol, 5.541 g) and ethanolamine (80 mmol, 4.838 mL) in absolute ethanol (20 mL) were heated to reflux at 100°C for 2 h, and then cooled. After that, the pure product compound **2** was obtained by suction filtration, and the yield was 98%.

## **2.2 Synthesis and characterization of 4-(4-vinylphenyl) morpholine (compound **4**)**

Methyltriphenylphosphine bromide (32 mmol, 11.335 g) and anhydrous tetrahydrofuran (20 mL) were added to the flask, bubbling nitrogen for 15 min, and then adding potassium tert-butoxide (32 mmol, 3.591 g) as catalyst for bubbling. Nitrogen was flushed for 30 min, and then compound **3** 4-(4-morpholine)-benzaldehyde (20 mmol, 3.825 g) was added to react overnight, and the reaction was stopped the next day. After dilution with n-hexane, suction filtration and drying were performed to obtain crude. The product was purified by column chromatography to obtain compound **4** as a white crystalline solid with a yield of 95%. <sup>1</sup>H NMR (400 MHz, CDCl<sub>3</sub>): δ 7.35 (s, 2H), 6.91 (s, 2H), 6.66 (s, 1H), 5.65 (s, 1H), 5.11 (s, 1H), 3.90 (s, 4H), 3.21 (s, 4H).

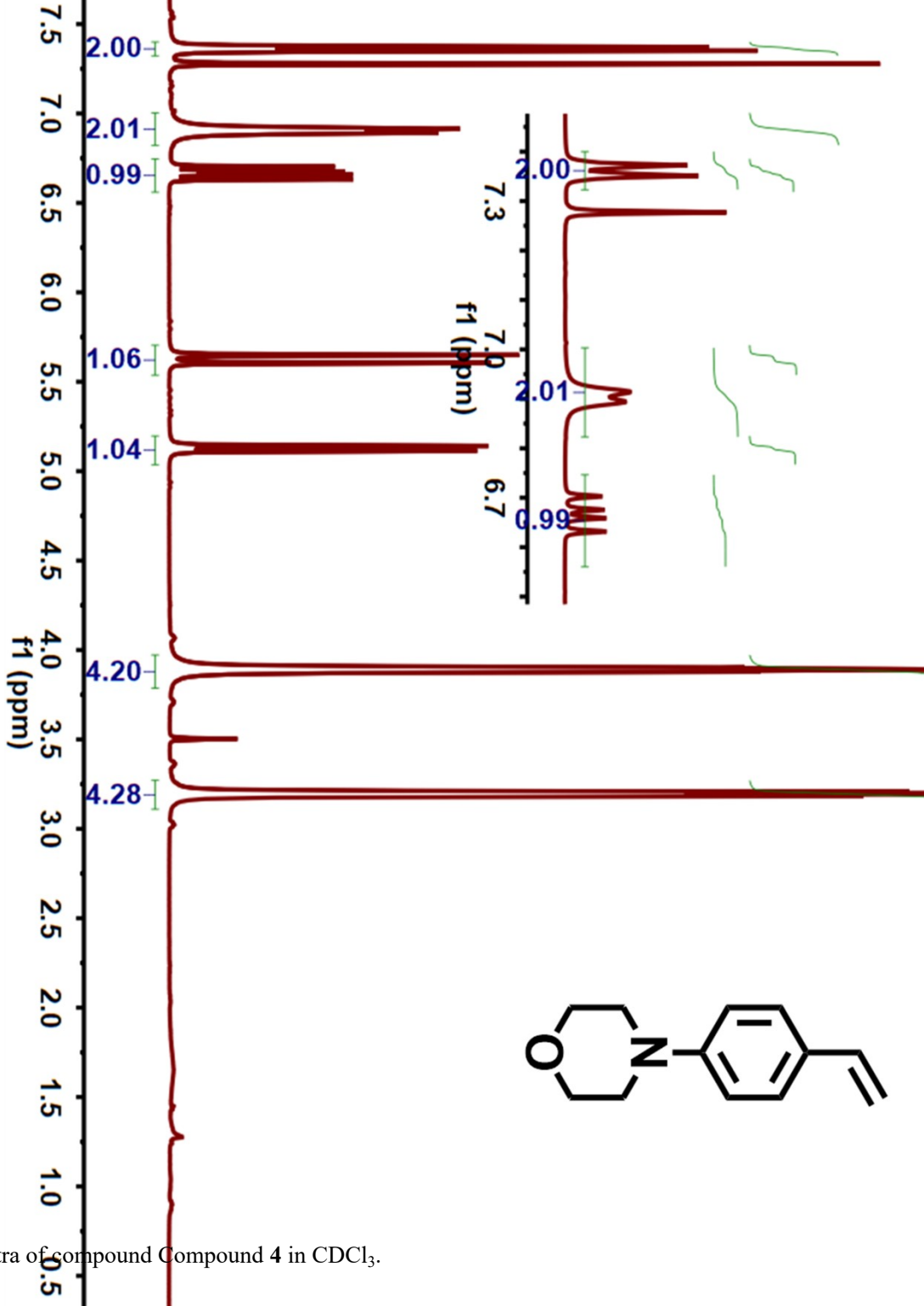


Fig. S1.  $^1\text{H}$  NMR spectra of compound Compound 4 in  $\text{CDCl}_3$ .

### 2.3 Synthesis and characterization of NAP-OH

Compound 2 (1.0 mmol, 0.3201 g) and compound 4 (1.5 mmol, 0.2839 g) were added to an eggplant flask and mixed with palladium acetate (0.2 mmol, 0.045 g) and tris (2-tolyl) phosphine (0.2 mmol, 0.061 g) as a catalyst, dissolved in a mixed solvent of acetonitrile (3 mL) and triethylamine (1 mL), heated under reflux at 105°C for 12 h to obtain a crude product. The crude product was purified by column chromatography in an eluent with a mixture of petroleum ether and ethyl acetate (2:1, v/v) to give the pure product NAP-OH as a red solid in 86% yield.  $^1\text{H}$  NMR (400 MHz,  $\text{DMSO}-d_6$ ):  $\delta$

8.96 (s, 1H), 8.52 (s, 1H), 8.45 (s, 1H), 8.20 (s, 1H), 7.98 (s, 1H), 7.87 (s, 1H), 7.73 (s, 2H), 7.55 (s, 1H), 7.02 (s, 2H), 4.84 (s, 1H), 4.16 (s, 2H), 3.76 (s, 4H), 3.64 (s, 2H), 3.22 (s, 4H).  $^{13}\text{C}$  NMR (101 MHz, DMSO)  $\delta$  164.08 (s), 163.78 (s), 151.80 (s), 142.04 (s), 135.65 (s) 131.64 – 130.72 (m) 129.25 (d,  $J = 8.1$  Hz) 128.66 (s) 127.72 (s), 127.14 (s), 122.9 (s), 58.30 (s), 48.01 (s), 42.1806, found: 42.1806.

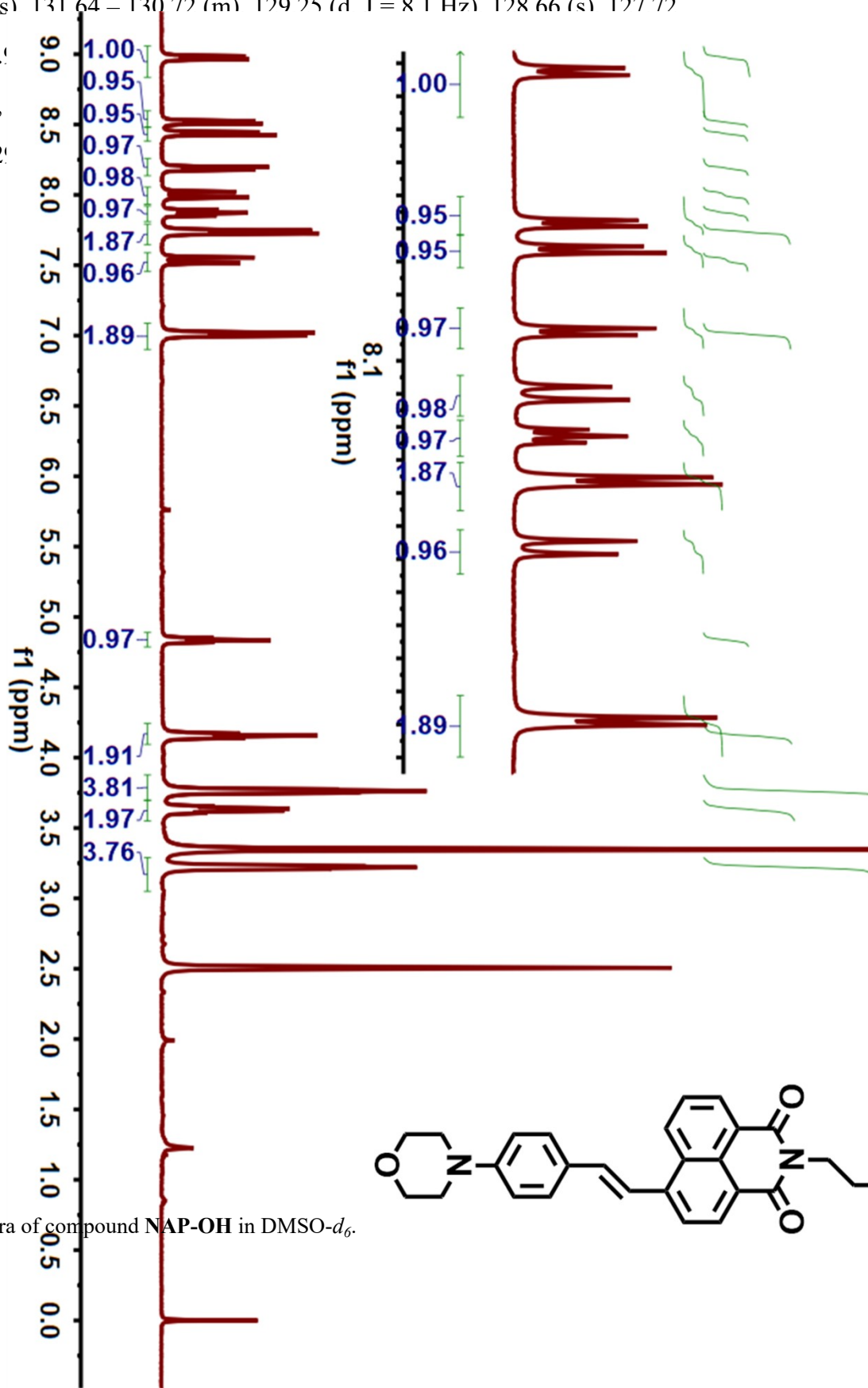


Fig S2.  $^1\text{H}$  NMR spectra of compound **NAP-OH** in  $\text{DMSO}-d_6$ .

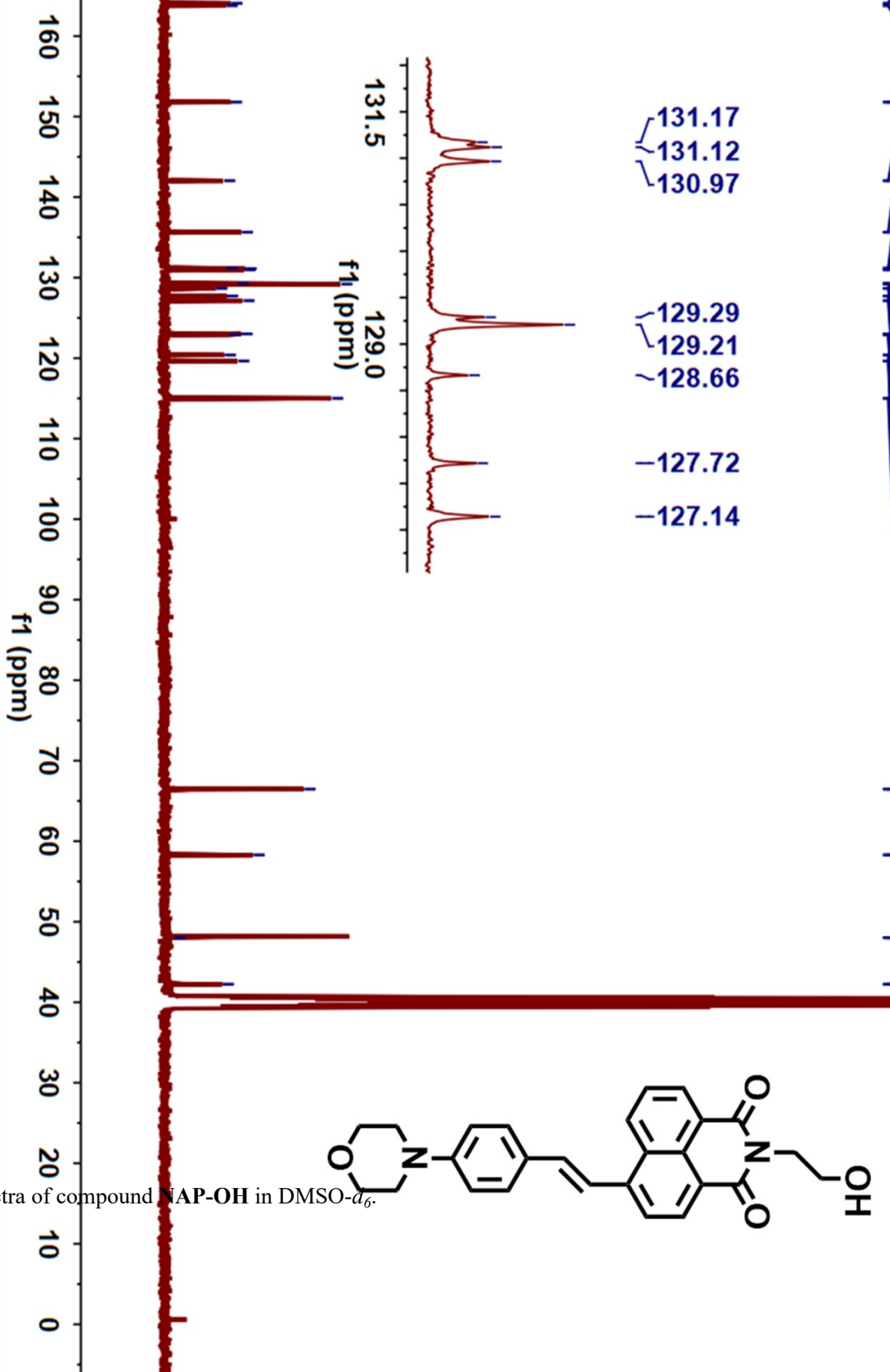


Fig. S3.  $^{13}\text{C}$  NMR spectra of compound NAP-OH in  $\text{DMSO}-d_6$ .

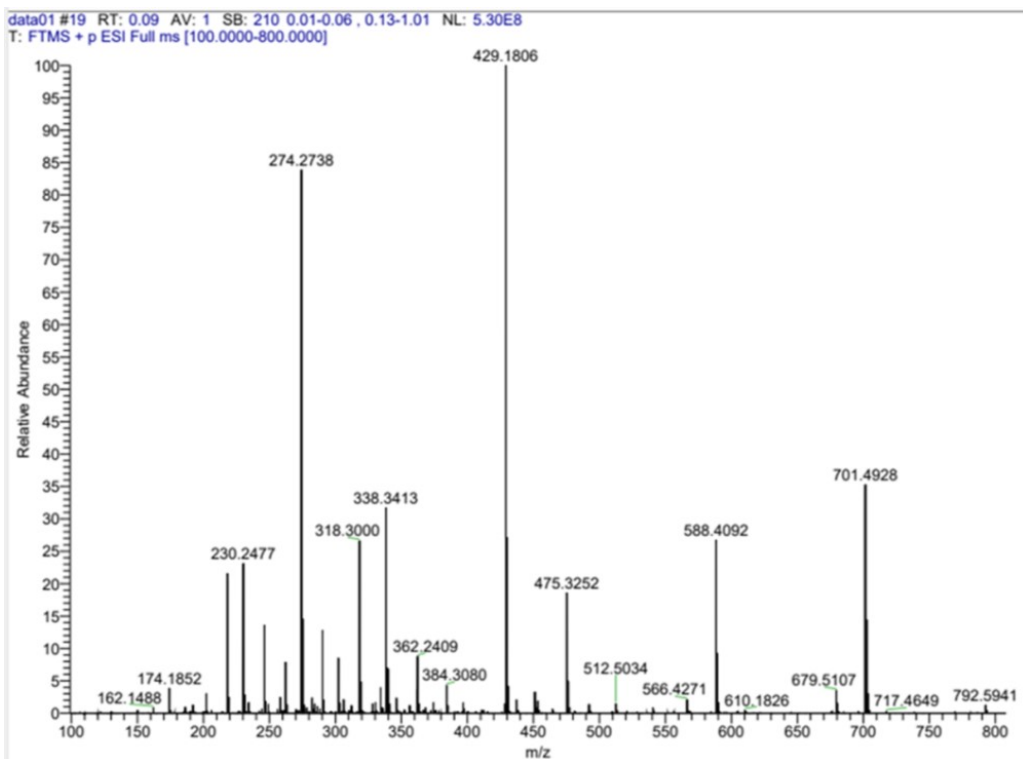


Fig. S4. HRMS spectra of compound NAP-OH.

### 3. The theoretical calculation

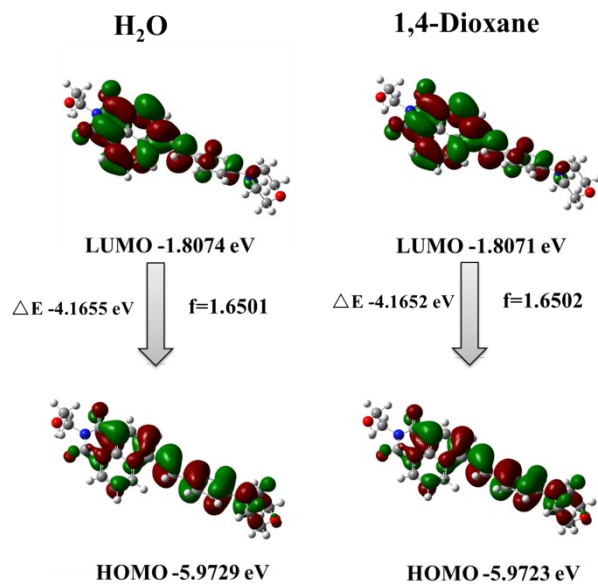


Fig. S5. TD-DFT calculation (B3LYP/6-31G\*, Gaussian 16) result of NAP-OH: energy diagram, Kohn-Sham HOMO and LUMO, ground state and excited state energy in  $\text{H}_2\text{O}$  and 1,4-Dioxane ( $\text{H}_2\text{O}$ :  $f$ : 1.6051; 1,4-Dioxane:  $f$ : 1.6052).

### 4. Determination water contents in various samples.

#### 4.1 Fluorescence emission spectroscopic studies of NAP-OH in organic solvents containing different amounts of water.

A solution of **NAP-OH** (1 mM, 30  $\mu$ L) dissolved in an organic solvent was added to an organic solvent-water mixture (2970  $\mu$ L) containing different moisture (0-100%, v/v). All fluorescence spectroscopic measurements of **NAP-OH** were done at 25 °C. Quenching efficiency (QE:  $1-I/I_0$ ) was reported as a function of [water].

#### **4.2 Determination of detection limit of NAP-OH toward water in organic solvents.**

The fluorescence emission spectrum of **NAP-OH** (10  $\mu$ M) in dry organic solvent was measured 10 times to determine the background noise  $\sigma$ . The fluorescence intensity was measured after adding various amounts of water from 0 to 10% (v/v) in a dry organic solvent. A linear regression curve was then fitted to the fluorescence intensity as a function of [water], and the slope of the curve was calculated. The detection limits were calculated by the equation,  $3\sigma/\text{slope}$ .

#### **4.3 Reproducibility of the sensor in 0.5% (v/v) H<sub>2</sub>O/1,4-Dioxane.**

Sample preparation: A solution of **NAP-OH** (1 mM, 30  $\mu$ L) dissolved in dry 1,4-Dioxane solvent was added to 1,4-Dioxane (2955  $\mu$ L) containing 15  $\mu$ L H<sub>2</sub>O. Final concentration of **NAP-OH** in solution was 10  $\mu$ M. Repeatability test: First, fluorescence measurements were performed immediately after thoroughly mixing 0.5% water with 1,4-dioxane containing **NAP-OH**. Second, a mixed solvent containing 0.5% water was added to calcium chloride for drying and the fluorescence test was performed immediately. Next, 0.5% water was added to the dried solvent and the fluorescence test was performed immediately. The above steps were repeated 6 times, and the fluorescence emission intensity at 622 nm was recorded each time( $\lambda_{\text{ex}} = 450$  nm, slit: 5/5 nm, voltage=600 V, 25°C). These results demonstrated that the method has good reproducibility for the quantification of water in organic solvents.

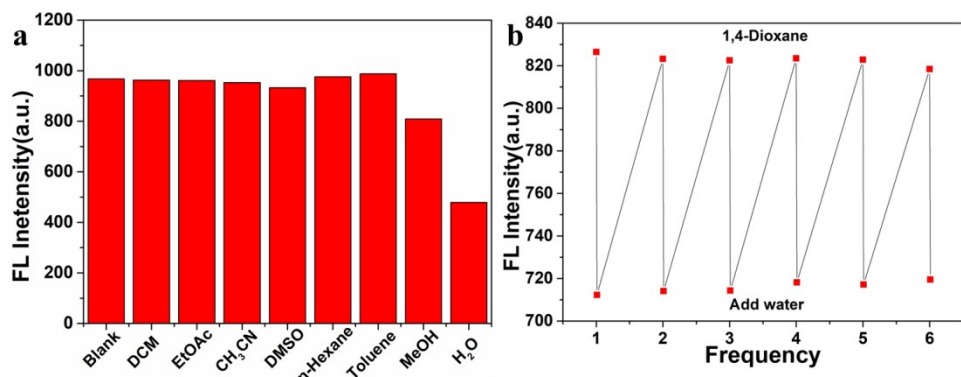
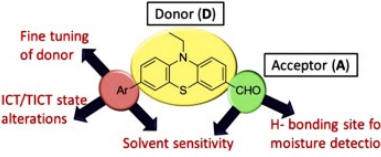
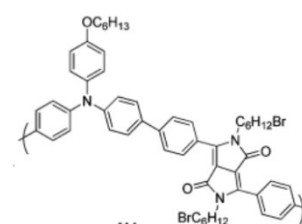
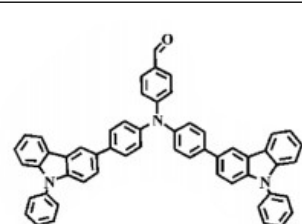
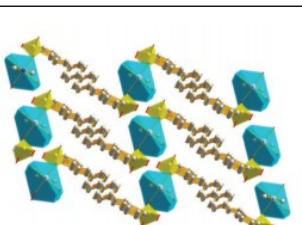


Fig. S6. (a) Fluorescence intensity of **NAP-OH** (10  $\mu$ M) in 1,4-Dioxane mixed with various organic solvents (1.00%, v/v); (b) the reproducibility of the **NAP-OH** in 0.5% (v/v) H<sub>2</sub>O/1,4-Dioxane at 25 °C.

**Table. S1** Comparison of trace water detection methods.

Sensors	Detecting system	Detection limit (ppm)	Linear scope (v/v %)	Reference
	1,4-Dioxane	54	0-1.4%	This Work
	Acetone	28	0-1.6%	
	THF	37	0-1.8%	
	THF	64	0-1.25%	10.1021/acs.analche.9b00032 [1]
	ACN	1920	0-1.25%	
	Acetone	420	0-2.5%	
	THF	1300	0-6.25%	10.1016/j.jphotochem.2020.11280 [2]
	ACN	400	0-6.25%	
	ACN	500	1-5%	10.1039/C8AN00450A [3]
	THF	500	0.3-5%	
	THF	280	0-0.38%	10.1016/j.dyepig.2020.108554 [4]
	ACN	130	0-0.38%	
	Acetone	210	0-0.38%	
	THF	80	0-1.32%	10.1016/j.jphotochem.2

	ACN	30	0-0.17%	020.112804 [5]
	DMSO	210	0-2.9%	
 N1	THF	50	0-2%	10.1039/c6n j00192k [6]
	THF	130	0-0.5%	10.1016/j.d yepig.2019. 03.008 [7]
	1,4-Dioxane	94	0-2.7%	10.1039/C8 TC04483J [8]

## 5. Cell co-staining experiments

**NAP-OH** was dissolved in dimethyl sulfoxide at a concentration of 1 mM. The cytotoxicity of **NAP-OH** on HeLa cells was detected by the mtt method. Live cell imaging, stained with 10  $\mu$ M **NAP-OH** for 30 min. Under a confocal laser scanning microscope (Leica SP8), **NAP-OH** was excited with a 405 nm laser with an emission wavelength of 650-750 nm.

Starvation experiment. HeLa cells were cultured under glucose starvation conditions for 24 h, then stained with **NAP-OH** (10  $\mu$ M, 30 min), washed with PBS, and imaged with a confocal microscope.

Co-localization experiments. HeLa cells were incubated with 10  $\mu$ M **NAP-OH** for 30 min. After washing with PBS, it was stained with BODIPY 493/503 (5  $\mu$ m, 10 min) or Lysotracker Green (50 nm, 10 min). After washing with PBS, cells were imaged with a confocal microscope.

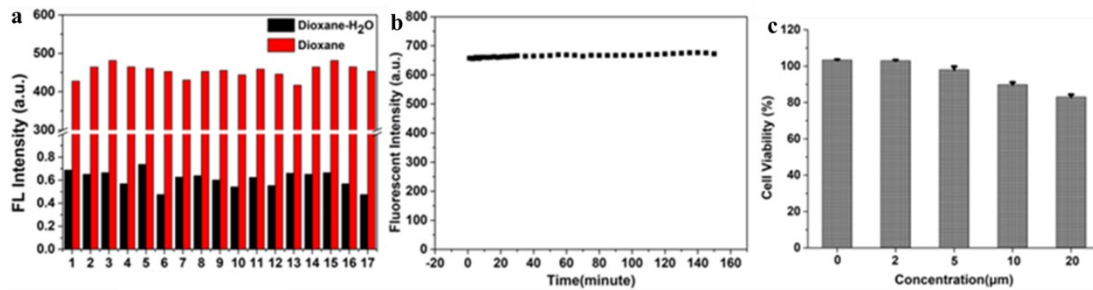


Fig.S7. (a) Selectivity of Probe **NAP-OH** (1: probe, 2: Cl<sup>-</sup>, 3: SO<sub>4</sub><sup>2-</sup>, 4: NO<sub>3</sub><sup>-</sup>, 5: Mg<sup>2+</sup>, 6: Na<sup>+</sup>, 7: Zn<sup>2+</sup>, 8: Al<sup>3+</sup>, 9: Ca<sup>2+</sup>, 10: Fe<sup>3+</sup>, 11: Fe<sup>2+</sup>, 12: Ser, 13: HClO, 14: H<sub>2</sub>O<sub>2</sub>, 15: Arg, 16: Cys, 17: GSH); (b) The photostability of **NAP-OH**; (c) Cytotoxicity of **NAP-OH**.

## References

- 1 F. Y . Wu, L. Y . Wang, H. Tang, D. R. Cao, Excited state intramolecular proton transfer plusaggregation-induced emission-based diketopyrrolopyrrole luminogen: photophysical properties and simultaneously discriminative detection of trace water in three organic solvents, *Anal. Chem.* **91** (2019) 5261-5269.
- 2 P . Majee, P . Daga, D. K. Singha, D. Saha, P . Mahata, S. K. Mondal, *J. Photochem. Photobiol., A.*, 2020, **402**, 112830.
- 3 S. Song, Y . Zhang, Y . Y ang, C. Wang, Y . Zhou, C, Zhang, Y . Zhao, M. yang, Q. Lin, *Analyst*, 2018, **143**, 3068-3074.
- 4 J. Nootem, C. Sattayanon, S. Namuangruk, P . Rashatasakhon, K. Chansaenpak, *Dyes. Pigm.*,2020, **181**, 108554.
- 5 T. Sachdeva, M. D. Milton, *J. Photochem. Photobiol., A.*, 2020, **402**, 112804.
- 6 L. Wang, L. yang, L. Li, D. Cao, *New. J. Chem.*, 2016, **40**, 6706-6713.
- 7 L. Chen, X. Tian, Y . Li, C. Yang, L. Lu, Z. Zhou, Y . Nie, *Dyes. Pigm.*, 2019, **166**, 1-7.
- 8 F. Cheng, R. Fu, Y u.Wen, Y . Y . Yang, C. Zeng, Y . Zhang, S. Hu, X. Wu, *J. Mater. Chem. C.*, 2018, **6**, 12341-12346.